

CHARACTERIZATION AND SIMULATION OF OPTICAL DELAY SYSTEM FOR THE PROOF-OF-PRINCIPLE EXPERIMENT OF OPTICAL STOCHASTIC COOLING AT IOTA*

A. J. Dick, P. Piot¹, Northern Illinois Center for Accelerator & Detector Development
Department of Physics, Northern Illinois University, DeKalb, IL, USA
J. Jarvis, Fermi National Accelerator Laboratory, Batavia, IL, USA
¹also at Argonne National Laboratory, Lemont, IL, USA

Abstract

The Optical Stochastic Cooling (OSC) experiment at Fermilab's IOTA storage ring uses two undulators to cool a 100 MeV electron beam over many turns. The radiation emitted by electrons in the first undulator is delayed and imaged in the second undulator where it applies a corrective energy kick on the beam. Imperfections in the manufacturing of the delay plates can lead to a source of error. This paper summarizes the experimental characterization of the absolute thickness of these delay plates using an interferometric technique. The measured "thickness maps" are implemented in the Synchrotron Radiation Workshop (SRW) program to assess their impact on the delayed radiation pulse. The procedure is outlined more fully in the technical note [1].

INTRODUCTION

Optical Stochastic Cooling (OSC) implemented in storage rings employs optical radiation to detect information on the beam distribution and apply a corrective kick [2]. Such a process is repeated multiple times as the stored beam circulated in the storage ring stochastically reducing the phase-space emittance. The optical signal is generated via undulator radiation as the beam passes through a "pickup" undulator. The radiation (possibly amplified) is imaged into a downstream "kicker" undulator where it is coupled to the beam to result in a corrective kick. A proof-of-principle experiment of OSC is currently in preparation at Fermilab's IOTA storage ring [3].

In its first phase, the experiment will implement a passive-OSC configuration where the radiation produced in the pickup undulator is directly imaged in the kicker undulator. In a subsequent phase, an "active"-OSC configuration will be examined where the radiation is first amplified before being imaged in the kicker undulator. The advantage of the active OSC is its ability to support larger corrective kicks and hence faster cooling rates. In both setups, the particle beam is separated from the optics through a bypass chicane and the arrival time of the radiation must match the particle-beam time of flight.

* This work is supported by U.S. Department of Energy under award No. DE-SC0013761 with Northern Illinois University and by the U.S. National Science Foundation under award PHY-1549132, the Center for Bright Beams. Fermilab is managed by the Fermi Research Alliance, LLC for the DOE under contract number DE-AC02-07CH11359.

Optical Delay System

Two 0.25-mm rotating glass plates will be inserted in the optics line so to provide a variable delay. By changing the angle of the glass plates, the optical path length experienced by the undulator radiation changes. The two plates are placed in a symmetrical configuration to minimize the transverse displacement of the photon beam as the delay (i.e. the angle of the plate) is varied. The maximum delay is limited to 0.648 mm and 2.0 mm for the for passive- and active-OSC configuration respectively by the particle-bypass beamline geometry. Figure 1 displays the location of the delay plates in the optical line between the pickup and the kicker undulators.

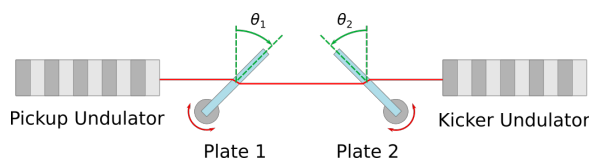


Figure 1: Configuration of the optical-delay system between pickup and kicker undulators.

To maximize the kick applied to the particle bunch in the kicker, the delay system operates with the plates near the Brewster's angle for the glass. This allows for the maximum transmission of p -polarized light. Additionally, the two plates are configured symmetrically to minimize the net horizontal displacement associated with the transmitted beam. Figures showcase the benefits of varying the plate anti-symmetrically: the net displacement vanishes, and the delay is a monotonic function of the angle.

The effective cooling range of the OSC setup requires the arrival of the particle beam and radiation to be within a quarter wavelength ($0.24 \mu\text{m}$ for passive-OSC). For this reason, the thickness of the plates must be close to the specified nominal value and have to be uniform over the entire surface. Nominally, the delay plates are $250 \mu\text{m}$ thick and made of CORNING-HPFS-7980 Glass. The purpose of this Note is to detail the experimental characterization of the delay plate using an interferometric technique and to document the possible impact on the undulator radiation properties for parameters consistent with the passive-OSC experiment at IOTA.

DELAY PLATES CHARACTERIZATION

Method

We used a Haidinger interferometer [4] system to measure the absolute thickness of each of the plates over the whole transverse profile; the experimental setup is described in Fig. 2. Haidinger's interference fringes refer to interference patterns in which coherent, monochromatic light incident on a thin film produces fringes at equal inclinations. The interference is a result of the reflection from the front and back faces of the thin film. The thickness of a sample can be determined from the fringe pattern if the index of refraction and wavelength of the incident light are known. The light reflected off the back surface of the sample will have a longer optical path length determined by the incident angle.

Assuming the sample thickness is slowly varying (no discontinuities) so that the two faces can be treated as parallel plates and that the thickness of the plate is relatively small, the fringe pattern as a function of viewing angle can be written as,

$$I(\theta) = I_0 \sin \left[2tn \cos \left(\frac{n}{n_{air}} \sin(\theta_i) \right) + \frac{\lambda}{2} \right], \quad (1)$$

where λ is the laser wavelength, I_0 the peak incident intensity, θ_i is the observation angle (same as the incident angle due to the law of reflection), $n = 1.4570$ is the index of refraction at $\lambda = 632.8$ nm, and t (the thickness of the plate) is a fitting parameter. The index of refraction is given by the Sellmeier equation where the coefficients (b_i and c_i , $i = 1, 2, 3$) are provided by the manufacturer.

Therefore, the only unknown parameter in Eq. (1) is the thickness t which can be inferred from a single-variable fitting function. It should be noted that we can only access the wrapped phase of the interference pattern. Phase information can be unambiguously determined using a second laser with a different wavelength on the same sample. However, it is shown later that the plates' thicknesses do not vary by more than a wavelength so that the phase does not need to be determined. Additionally, the absolute thickness is less important than the relative "flatness" of the plate, because an error of an integer-multiple of the laser wavelength can be corrected by rotating the plates; see Section . The primary concern is a steering error or focusing effect caused by an uneven plate.

Experimental Setup

The interferometer setup was taken from a paper on measuring the thickness of parallel glass plates[5] but used a single wavelength because the refractive properties of the glass are known. The laser is a 632.8 nm HeNe laser and the optical setup includes two collimating lenses, a 50/50 beamsplitter, a focusing lens, and a FLIR BLACKFLY CCD camera.

Figure 2(a) shows the interferometer setup used to characterize the plates. Each glass plate was placed at the focal point of the primary lens and mounted on a motorized translation stage which moves in the $x-y$ plane. The measurement

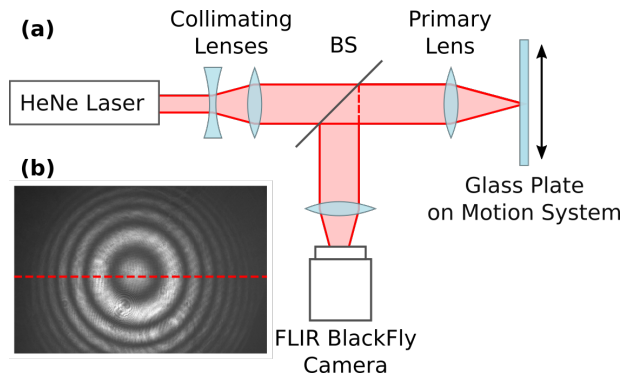


Figure 2: (a) Schematic of the Haidinger interferometer constructed to measure the plate thickness. (b) Measured interference-fringe pattern recorded on the CCD camera.

was automatized by a script that performed a 2-D scan of the plate across the laser spot. For each position, the fringe pattern is recorded with the CCD camera. An example of observed interference fringes appears in Fig. 2(b).

The interference-fringe pattern is measured using a FLIR BLACKFLY CCD camera. The camera consists of an array of 1920×1200 pixels with an individual size of $5.86 \mu\text{m}$. The fringe pattern described by Eq. (1) is a 1-dimensional function of the observation θ so the image must be processed before it is fit. First, a line-out along the center of the pattern is taken [along the red dashed line in Fig. 2(b)] then the pixel size is converted into an angle using the magnification of the optical line from the sample to the CCD

$$\theta = \tan^{-1} \left(\frac{\text{pixel} \times 5.86 \mu\text{m}}{Mf} \right), \quad (2)$$

where f is the focal length of the focusing lens and M the magnification of the system from the beam-splitter to the camera. Finally, the data are fitted to the fringe equation multiplied by a Gaussian profile describing the beam's transverse distribution (that is I_0 in Eq. (1) is taken to be a Gaussian function of θ). An example of analysis appears in Fig. 3.

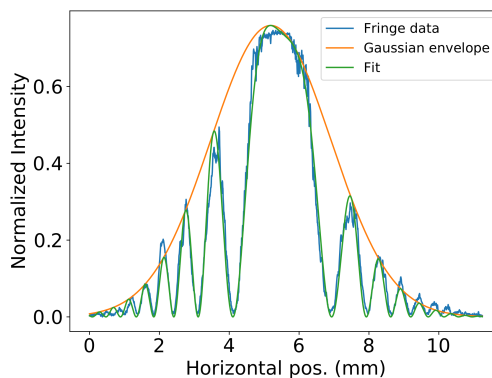


Figure 3: Measure interference-fringe pattern (blue trace) with fitted Eq. (1) (green trace) assuming a Gaussian-profile for the laser beam (orange trace).

Measurement Results

There were a total of 18 plates that were measured by this technique. Each plate was cataloged and stored so that it could be later matched with its measured profile. The average and root-mean-square (RMS) thickness of each plate measurement is shown in Fig. 4. A PYTHON script using a fitting routine from the SCIPY module was employed to fit the fringe equation defined in Eq. (1) and a Gaussian envelope to the data. The process was repeated over a 22 mm × 12 mm area of the plate surface so to provide a thickness map of the surface area; see Fig. 5.

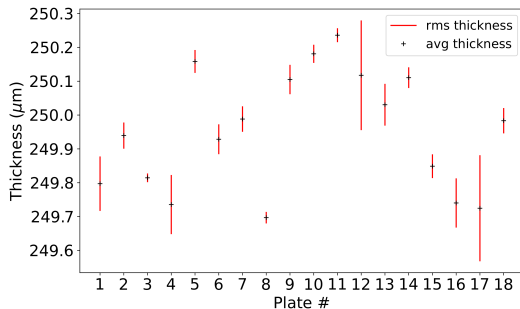


Figure 4: Average (blue circle) and RMS (red line) thickness associated with each of the 18 plates measured. The average and RMS values are computed over the 22 mm × 12 mm scanned plate surface.

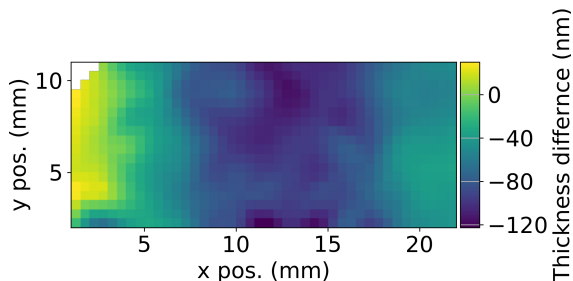


Figure 5: Transverse thickness profile of plate #2 as it varies from the nominal thickness of 250 μm.

IMPACT ON UNDULATOR RADIATION

SYNCHROTRON RADIATION WORKSHOP (SRW) is a wave-optics simulation program including simulation of synchrotron radiation from first principle [6]. We used SRW to simulate and propagate the undulator radiation through the optical delay line in the OSC experiment. In brief, undulator radiation from a 100 MeV electron traveling through the OSC undulator is generated and propagates the wavefront through the optical beamline consisting of a single-lens imaging (located at $z_l = 183$ cm from pick-up undulator center with focal length $f = 85$ cm) and two delay plates. The parameters of the undulators used to simulate the radiation are listed in Table 1.

Table 1: Undulator Parameters and Corresponding Radiation Wavelength for an Electron-Beam Energy of 100 MeV

Parameter	Passive OSC	Active OSC
Undulator parameter K	1.003	1.038
Undulator period (mm)	48.40	110.63
Number of periods	16	7
Radiat. wavelength (μm)	0.95	2.2

This simulation allows us to examine the difference between an ideal 250-μm delay plate and each of the measured plates. The procedure consist in first producing a transmission element of 250 μm (with idealized parallel faces) and the same optical properties as the delay-plate material and extracting the phase and intensity of the wavefront at its image point in the undulator. In subsequent simulations the measured transverse-thickness profile associated with each plate is used to create a realistic transmission elements for each of the plates. The imaged radiation field is then compared to the one associated with the idealized plates. Specifically, difference phase and intensity maps between the radiation field produced by the idealized and measured plate at the focal point are produced. Figure 6 displays snapshots of the undulator-radiation transverse optical-field distribution at the beginning, center, and end of the kicker undulator. The results indicate that the relative intensity variation over the transverse radiation spot is less than ~ 4% and the maximum phase difference below $\sim 2 \times 10^{-3}$ rad. These measurements confirm that the plate quality is sufficient to have minimal impact on the OSC experiment.

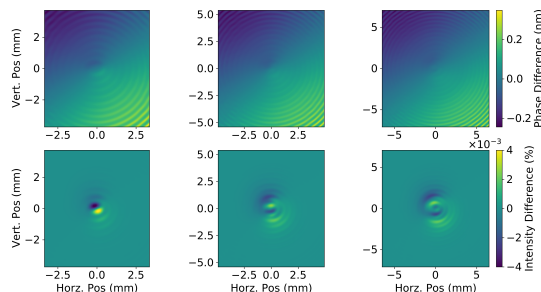


Figure 6: Effects of errors in a single plate on radiation in the kicker undulator.

SUMMARY

The thickness associated with the plates used to introduce a variable delay in the IOTA OSC experiment has been characterized and found to be 221 nm on average. SRW was employed to explore the impact on the imaged undulator radiation and confirms that the intensity and phase variation of the radiation transverse distribution is small (percent level on the intensity and sub- 5×10^{-3} rad for the phase variation). These results will be included in the start-to-end simulation of the OSC process for precise simulations.

REFERENCES

- [1] A. J. Dick, J. Jarvis, and P. Piot, “Characterization of the sub-mm delay plates for the iota optical-stochastic-cooling experiment”, FERMILAB, Batavia, IL, USA, Tech. Rep. FERMILAB-FN-1130-AD, 2021.
- [2] M. S. Zolotarev and A. A. Zholents, “Transit-time method of optical stochastic cooling”, *Phys. Rev. E*, vol. 50, pp. 3087–3091, Oct. 1994. doi:10.1103/PhysRevE.50.3087
- [3] V. Lebedev, J. Jarvis, H. Piekarz, A. Romanov, J. Ruan, and M. Andorf, “Conceptual design report: Optical stochastic cooling at iota”, 2021. arXiv: 2012.09967
- [4] E. A. de Oliveira and J. Frejlich, “Thickness and refractive index dispersion measurement in a thin film using the haidinger interferometer”, *Appl. Opt.*, vol. 28, no. 7, pp. 1382–1386, Apr. 1989. doi:10.1364/AO.28.001382
- [5] J.-A. Kim, J. W. Kim, C.-S. Kang, J. Jin, and J. Y. Lee, “An interferometric system for measuring thickness of parallel glass plates without 2π ambiguity using phase analysis of quadrature haidinger fringes”, *Rev. Sci. Instrum.*, vol. 88, no. 5, p. 055 108, May 2017. doi:10.1063/1.4983314
- [6] O. Chubar, A. Fluerasu, L. Berman, K. Kaznatcheev, and L. Wiegart, “Wavefront propagation simulations for beamlines and experiments with ‘Synchrotron Radiation Workshop’”, *J. Phys. Conf. Ser.*, vol. 425, no. 16, p. 162 001, 2013. doi:10.1088/1742-6596/425/16/162001